Separation Science and Technology
Publication details, including instructions for authors and subscription information:
http://www.informaworld.com/smpp/title~content=t713708471

Membrane extraction for sulfanilic acid removal from waste water

Yujun Wang[a]; Guangsheng Luo[a]; Weibin Cai[a]; Yan Wang[a]; Youyuan Dai[a]
[a] Chemical Engineering Department, Tsinghua University, Beijing, People's Republic of China

Online publication date: 24 April 2002

To cite this Article Wang, Yujun , Luo, Guangsheng , Cai, Weibin , Wang, Yan and Dai, Youyuan(2002) 'Membrane extraction for sulfanilic acid removal from waste water', Separation Science and Technology, 37: 5, 1163 — 1177
To link to this Article: DOI: 10.1081/SS-120002248
URL: http://dx.doi.org/10.1081/SS-120002248

SEPARATION SCIENCE AND TECHNOLOGY, 37(5), 1163–1177 (2002)

MEMBRANE EXTRACTION FOR SULFANILIC ACID REMOVAL FROM WASTE WATER

Yujun Wang,* Guangsheng Luo, Weibin Cai, Yan Wang, and Youyuan Dai

Chemical Engineering Department, Tsinghua University, Beijing 100084, People's Republic of China

ABSTRACT

The flow characteristics in hollow fiber modules (HFMs) were studied using resident time distribution (RTD) curves, which showed that the actual flow was nonideal and conformed to neither the ideal plug flow nor the complete mixed-flow models. Axial dispersion was found to decrease with an increase in flow velocity on the tube side and to increase with an increase in flow velocity on the shell side. Good agreement between the curves calculated using an axial diffusion model and experimentally determined RTD curves showed that the diffusion model can be used to describe the mass transfer characteristics in HFMs. In the study using 20% trioctylamine + 30% octanol + 50% kerosene–sulfanilic acid–water as actual extraction process, it was found that axial dispersion was the cause of the significant decrease in mass transfer performance. The resistance to mass transfer is located mainly in the boundary layer of aqueous phase. The large

*Corresponding author. Fax: (861) 062-770304; E-mail: wangyj97@mails.tsinghua.edu.cn

amount of treatment suggested that sulfanilic acid removal from its wastewater by HFM was an efficient process.

Key Words: Membrane extraction; Hollow fiber module; Sulfanilic acid; Axial diffusion model

INTRODUCTION

Textile dye industry wastes are characterized by strong color, high biochemical oxygen demand (BOD), high chemical oxygen demand (COD), high total organic carbon (TOC), and suspended solids (1,2). Especially, the organic compounds containing amino group and sulfonic group such as sulfanilic acid and *p*-amine naphthalene sulfonic acid are very difficult to deal with. The recovery of dye from its waste effluents has been accomplished mainly by oxidation, biodegradation, and adsorption on active carbon or polymeric resins.

Recently, membrane-separation processes such as reverse osmosis, ultrafiltration, and nanofiltration have been applied to treat the textile dye wastewater since they can reduce the volume of wastewater and recover valuable components from the waste stream (1).

Membrane extraction is a combinational technology of membrane separation and liquid–liquid solvent extraction. In recent years, it has been of significant interest to study the nondispersion membrane-extraction process using microporous membranes to immobilize the interfaces. It presents advantages of no entrainment, no flooding, very large interfacial area, and the possibility to realize extreme phase ratios (3) and has been applied to organic extraction (4,5), metal ions extraction (6,7), and fermentation products refinery (8). In this work, membrane extraction by hollow fiber module (HFM) was used for treatment of wastewater from textile dye industry.

An HFM is one of the typical membrane contactors in membrane extraction, in which hundreds or even thousands of hollow fibers are usually packed in random. Chen et al. (9) showed by theoretical calculation that the random packing had a great effect on the uneven flow in the shell. Their experimental results indicated that 50% of the fluid flowed through only 20% of the total cross-area. Park et al. (10) have shown that a significant degree of nonuniformity occurs in the flow distribution in the lumen side of a HFM by a finite-difference numerical method calculation and by tracer experiments. The nonuniformity of velocity reduced the efficiency of mass transfer in HFMs. The complicated calculation methods in the above-mentioned work has prompted the search for a simple mathematical model to describe the effects of the nonuniformity of velocity on mass transfer performance.

In the work discussed in this paper, tracer tests were used to examine flow characteristics and the actual membrane-extraction process was used to study the influence of nonideal flow on the mass transfer characteristics.

EXPERIMENTAL

Distribution Coefficient Determination

The actual membrane-extraction system used was 20% triotylamine + 30% octanol + 50% kerosene–*p*-amine benzene sulfonic acid–water. Octanol was added to avoid formation of a third phase. Kerosene was a commercially available solvent. Sulfanilic acid was dissolved in distilled water to different final concentrations. Sulfuric acid or sodium hydroxide was used for pH adjustment.

A measured volume of 20 or 25 mL solvent was mixed with 50 mL aqueous solution for over 2 hr on the shaking table at 25°C. The equilibrium concentration of sulfanilic acid in aqueous phase was determined with a HP8452 UV spectrophotometer (Hewlett Packard, Waldbronn, Germany) at 215 nm.

Determination of Flow Status

Figure 1 shows a schematic representation of the experimental setup used for the determination of residence time distribution (RTD) curves. A step-trace method using saturated KCl solution as tracer was applied to examine the flow status in the HFMs. For the determination of shell-side flow, the tracer solution was pumped through the shell side of the module and the tube side was filled with

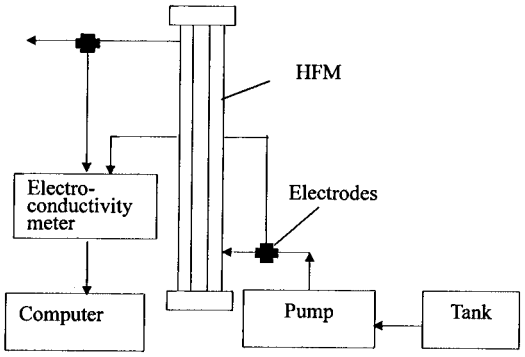

Figure 1. Schematic of experimental setup for RTD curve determination.

solvent. For the determination of tube-side flow, the tracer solution was pumped through the tube side and the shell side was filled with solvent. The concentrations at the module inlet and outlet were monitored on-line with electro-conductivity meters.

The polypropylene HFMs used in this work were manufactured by Seawater Desalting Center of National Ocean Agency in Tianjin, China. The characteristics of these modules are shown in Table 1.

Membrane-Extraction Procedure

When extraction was carried out in a module, the aqueous phase flowed through the tube side, and the organic phase flowed counter-currently in the shell side. To avoid the breakthrough of the solvent, the pressure of the aqueous phase was 10 kPa higher than that of the organic phase. Samples at the module inlet and outlet under steady state were collected and the concentration was determined. The concentration of the sulfanilic acid was determined using a HP8452 UV spectrophotometer at 215 nm. The loaded solvent was regenerated with 10%(w/w) sodium hydroxide solution.

THEORETICAL

Calculation of Axial Diffusion Coefficient Pe Without Mass Transfer

According to the mass conversation principle, the axial diffusion equation can be written as Eq. (1).

$$\frac{\partial C}{\partial \theta} = \left(\frac{E_z}{uL}\right)\frac{\partial^2 C}{\partial Z^2} - \frac{\partial C}{\partial Z} = \frac{1}{\mathrm{Pe}}\frac{\partial^2 C}{\partial Z^2} - \frac{\partial C}{\partial Z} \tag{1}$$

Table 1. Characteristics of Hollow Fiber Modules

No.	Module Length (cm)	Module Diameter (cm)	Fiber Number	Inner Diameter d_i (mm)	Thickness of Fiber (mm)	Porosity of Fiber ϵ
A	33.5	3.32	3400	0.40	0.04	0.55
B	33.5	3.32	2500	0.40	0.04	0.55

MARCEL DEKKER, INC.
270 Madison Avenue, New York, New York 10016

where

$$C = \frac{c}{c_0}, \quad \theta = \frac{t}{\tau}, \quad Z = \frac{z}{L} \tag{2}$$

Pe being the only unknown parameter was determined using the stimulus–response curves.

Calculation of True Mass Transfer Coefficients by Axial Diffusion Model

According to the axial diffusion model, Eq. (3) is the differential equation group for the two phases.

$$\frac{d^2X}{dZ^2} - \mathrm{Pe_x}\frac{dX}{dZ} - N_x\mathrm{Pe_x}(X - X^*) = 0 \tag{3}$$

$$\frac{d^2Y}{dZ^2} + \mathrm{Pe_y}\frac{dY}{dZ} + N_x \cdot \frac{u_x}{u_y}\mathrm{Pe_y}(X - X^*) = 0$$

The boundary conditions are:

$$Z = 0 \qquad\qquad Z = 1 \tag{4}$$

$$-\frac{dC_x}{dZ} = \mathrm{Pe_x}B(1 - C_{x,z=0^+}) \qquad -\frac{dC_x}{dZ} = 0$$

$$-\frac{dC_y}{dZ} = 0 \qquad\qquad -\frac{dC_y}{dZ} = \mathrm{Pe_y}(C_{y1} - C_{y,z=1})$$

The finite-difference method was used to solve the above equation group. When $\mathrm{Pe_x}$, $\mathrm{Pe_y}$, C_{x0}, C_{x1}, C_{y0}, and the distribution coefficient m are known, the true mass transfer unit can be obtained. In this paper, m, C_{x0}, C_{x1}, and C_{y0} were determined by experiments and $\mathrm{Pe_x}$ and $\mathrm{Pe_y}$ were obtained from the RTD curve.

Calculation of Apparent Mass Transfer Coefficients

The apparent mass transfer coefficients are the overall mass transfer coefficients obtained under the condition of plug flow. These can be obtained from correlation (5).

Here, the inlet and outlet concentrations of aqueous phase can be measured. The distribution coefficient m of the experimental system is variable with the

MARCEL DEKKER, INC.
270 Madison Avenue, New York, New York 10016

equilibrium pH and concentration. For simplification, the average distribution coefficients were used to calculate the apparent mass transfer coefficients.

$$K_{aq} = \frac{Q_{aq}}{A} \cdot \frac{1}{1 - Q_{aq}/mQ_0} \ln \frac{C_{x0} - C^*_{x0}}{C_{x1} - C^*_{x1}} \tag{5}$$

RESULTS AND DISCUSSION

Liquid–Liquid Equilibrium

The dissociation of sulfanilic acid in aqueous solution can be described as follows:

$$NH_3^+ - Ar - SO_3H \overset{K_1}{\leftrightarrow} NH_3^+ - Ar - SO_3^- + H^+ \tag{6}$$

$$NH_3^+ - Ar - SO_3^- \overset{K_2}{\leftrightarrow} NH_2 - Ar - SO_3^- + H^+$$

The solute has three different forms under different pH of the solution, which were designated as A^+, $A^{\pm}$, and A^-, respectively. The influence of pH on the distribution coefficients is shown in Fig. 2. When the equilibrium pH is below 1 or above 5, A^+ or A^- will be the major existent solute. Since the extractant trioctylamine mainly combines with $A^{\pm}$, a small distribution coefficient will be obtained in the above two cases. Only when the equilibrium pH is between 2 and 5 can a large distribution coefficient be obtained.

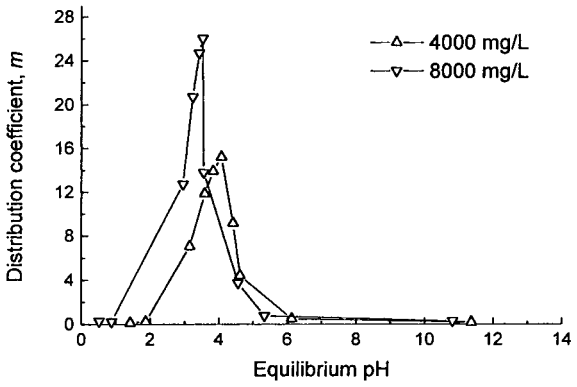

Figure 2. Effects of equilibrium pH on distribution coefficient under different initial solute concentrations.

MARCEL DEKKER, INC.
270 Madison Avenue, New York, New York 10016

Table 2. Effect of Initial Concentration on Distribution Coefficients Without pH Adjustment

Initial Concentration (mg/L)	Equilibrium Concentration (mg/L)	Phase Ratio	Distribution Coefficients (m)
8000	701.2	1:2.5	26.03
4000	564.1	1:2.5	15.23
2500	432.8	1:2	9.55
1000	251.9	1:2	5.94
200	95.3	1:2	2.21
120	70.2	1:2	1.42

Data given in Table 2 indicated the effect of the initial concentration in the aqueous phase on liquid–liquid equilibrium. The distribution coefficients increased with an increase in the initial concentration of aqueous phase.

Effect of Flow Rate and pH on Mass Transfer

The flow rate of one phase was fixed to study the effects of flow rate of another phase on the mass transfer. As shown in Fig. 3, under a certain velocity of

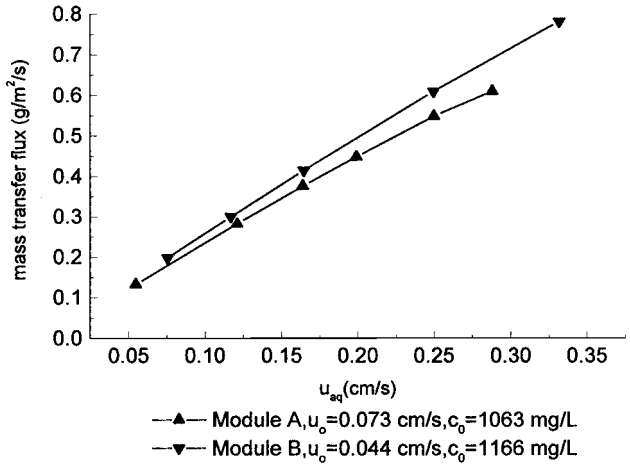

Figure 3. Effect of the velocity of aqueous phase on mass transfer flux.

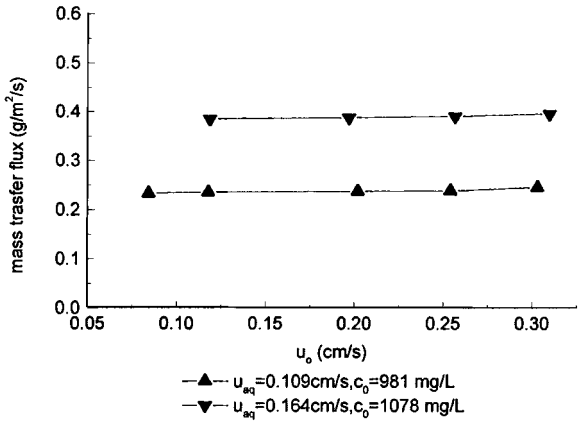

Figure 4. Effect of the velocity of organic phase on mass transfer flux in Module A.

the organic phase the mass transfer flux in modules A and B increased linearly with an increase in flow velocity of aqueous phase. It was the thinner boundary layer in the aqueous phase under higher flow rate that improved the mass transfer flux. The mass transfer flux did not increase significantly when the flow rate of the organic phase was increased under a fixed velocity of aqueous phase (Fig. 4),

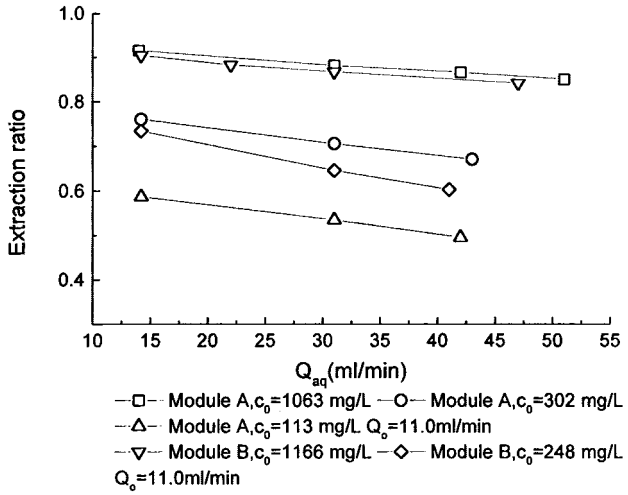

Figure 5. Effects of the flow rate of aqueous phase on extraction ratio under different initial concentrations.

MARCEL DEKKER, INC.
270 Madison Avenue, New York, New York 10016

Table 3. Effect of pH on Extraction Ratio

Module A				Module B			
Initial Concentration (ppm)	Feed pH	Raffinate pH	Extraction Ratio	Initial Concentration (ppm)	Feed pH	Raffinate pH	Extraction Ratio
98.1	2.65	6.56	0.566	596.3	1.86	5.69	0.823
98.1	3.21[a]	6.85	0.604	596.3	2.86[a]	6.04	0.845
98.1	3.56	6.94	0.600	596.3	2.97	7.17	0.772
98.1	3.82	7.29	0.316	596.3	11.69	11.60	0.010

[a] Initial pH.

which suggested that the resistance to the mass transfer was located mainly in the boundary layer of aqueous phase.

When the flow rate of aqueous phase increased, the total amount of solute to be removed increased more sharply than the mass transfer coefficients did. Therefore, a relatively low extraction ratio was obtained under high velocity of aqueous phase (Fig. 5). At the same time, the removal efficiency increased with an increase in the initial concentration of the aqueous phase. After extraction three times, the outlet concentration reached 60 mg/L with the initial concentration of about 1000 mg/L and the phase ratio of 1:4, indicating that HFM extraction was an efficient process for sulfanilic acid removal.

As shown in Table 3, the initial pH of the aqueous phase influenced the extraction ratio greatly because it influenced the distribution coefficients greatly. The highest extraction ratio was obtained without pH adjustment of the initial solution. The extraction ratio decreased slowly upon sulfuric acid addition while it decreased abruptly upon basic solution addition.

Typical Resident Time Distribution Curves of Shell Side and Tube Side

The RTD curves given in Fig. 6 show that the actual flow status in the tube side conformed to neither an ideal plug flow nor a complete mixed-flow model. In fact, there existed back mixing and forward mixing due to the drag associated with the inner wall of the fibers. The randomly packed and twisted fibers resulted in resistance gradients through the fiber bundles. The distribution of velocity on the tube side was therefore nonuniform. The RTD curves given in Fig. 7 show more complicated flow characteristics for the shell side than for the tube side.

MARCEL DEKKER, INC.
270 Madison Avenue, New York, New York 10016

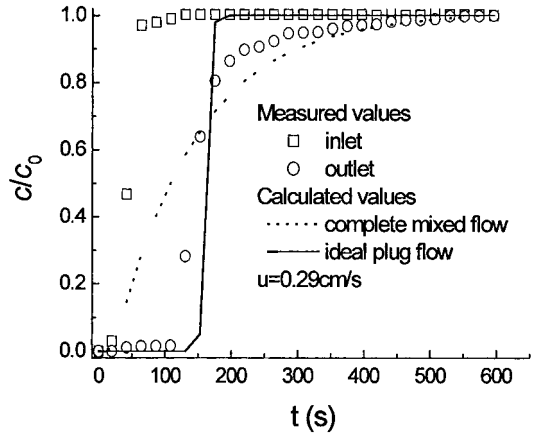

Figure 6. The RTD curves of tube side in Module B.

Compared to the case for ideal plug flow, "dead zones" and channeled flow were observed. The locations of the inlet and outlet of the module meant that fluid had to flow across the fiber bundles to be distributed evenly at the cross-section. As a result of the larger resistance across than along the fibers, the fluid tended to flow along the fibers thereby causing an uneven cross-sectional velocity profile. In addition, the nonuniform packing of the modules meant that the fibers were not all straight and parallel. This arrangement, by causing channel variations along

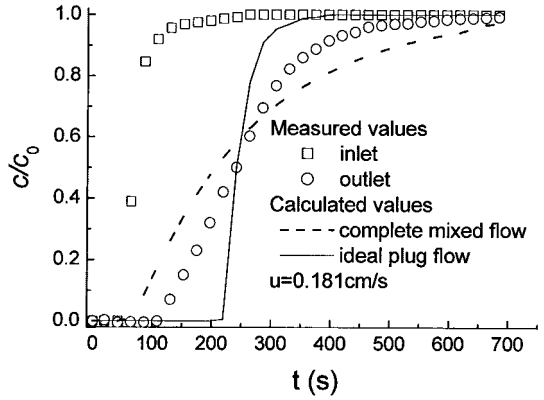

Figure 7. The RTD curves of shell side in Module A.

MARCEL DEKKER, INC.
270 Madison Avenue, New York, New York 10016

the length of the fiber bundle, resulted in cross-flow. The fluid tended to favor passage through the channels with large equivalent diameters. The uneven flow observed was clearly a result of the random packing of fiber bundles.

Comparison of the Calculated Curves and Experimental Curves

Figure 8 shows that there was good agreement between the experimentally determined curves and those calculated using the diffusion model. The axial diffusion model in which all the nonideal factors contribute to axial dispersion has been applied widely for the design of reactors and extraction columns. These results show that this model can be used to describe the flow characteristics in HFMs.

Influence of the Velocity to the Axial Diffusion

Figure 9 shows that velocity affects the axial dispersion significantly. On the shell side, the resistance to flow of the fluid across the fibers increased with increased velocity. For paths far from the inlet, lower velocities caused severe bypassing, resulting in an increase in axial dispersion. On the tube side, the influence of the drag associated with the fiber inner wall was reduced as the velocity increased. At the same time the increase in the radial mixing in each fiber, giving a more even flow distribution, resulted in a decrease in axial dispersion.

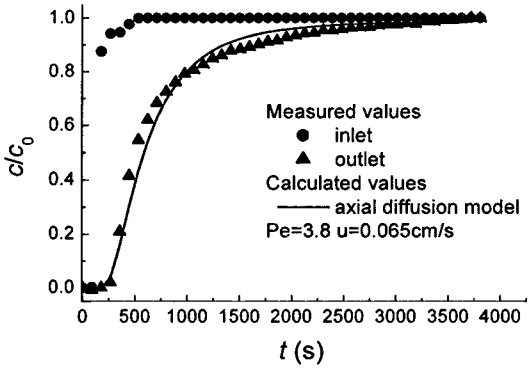

Figure 8. Comparison of experimental RTD curves and calculated ones of shell side in Module B by axial diffusion model.

MARCEL DEKKER, INC.
270 Madison Avenue, New York, New York 10016

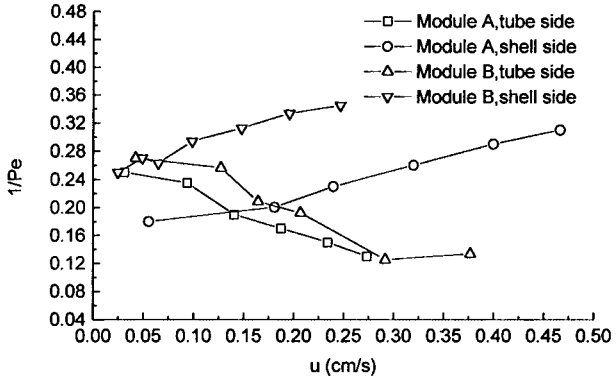

Figure 9. Influence of velocity to axial diffusion.

Comparison of the True and the Apparent Mass Transfer Coefficient

Figure 10 shows that the true mass transfer coefficient obtained by solving the axial diffusion equation was larger than the apparent coefficient. This indicated that the mass transfer performance was inhibited by axial back mixing. This is borne out by examination of an actual concentration profile in a HFM, given in Fig. 11. The observed concentration jump at the module inlet and outlet would reduce the concentration driving force and thus reduce mass transfer performance.

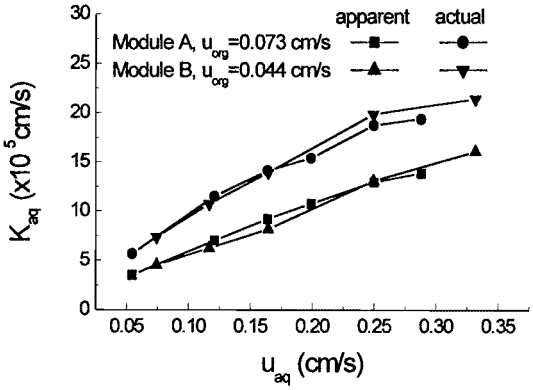

Figure 10. Comparison of the apparent and the actual mass transfer coefficients.

MARCEL DEKKER, INC.
270 Madison Avenue, New York, New York 10016

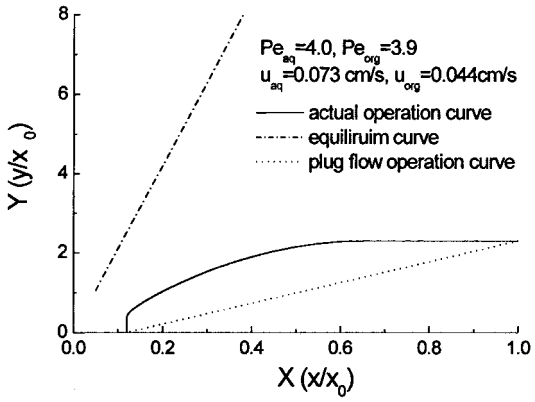

Figure 11. Actual concentration profile in Module B.

CONCLUSIONS

The flow characteristics in HFMs were studied using RTD curves. They showed that the actual flow was nonideal and conformed to neither the ideal plug flow nor the complete mixed-flow models. Axial dispersion was found to decrease with an increase in flow velocity on the tube side and to increase with an increase in flow velocity on the shell side. Good agreement between the curves calculated using an axial diffusion model and experimentally determined RTD curves showed that the diffusion model can be used to describe the mass transfer characteristics in HFMs.

Using 20% trioctylamine + 30% octanol + 50% sulfanilic acid–water as experimental system, the mass transfer characteristics of membrane-extraction process have been studied in the hydrophobic polypropylene HFMs. The results suggested that sulfanilic acid removal from its wastewater by HFM was an efficient process. The resistance to mass transfer was located mainly in the boundary layer of aqueous phase. The removal ratio was influenced by the flow rate of two phases, the pH, and the initial concentration of the aqueous phase. It was found that axial dispersion was the cause of the significant decrease in mass transfer performance.

NOMENCLATURE

A mass transfer surface area (cm^2)
c concentration (mg/L)
C dimensionless concentration

MARCEL DEKKER, INC.
270 Madison Avenue, New York, New York 10016

d diameter (cm)
E axial diffusion number (cm^2/sec)
L length of the module (cm)
K overall mass transfer coefficients (cm/sec)
N number of mass transfer unit
Q the flow rate (mL/sec)
t time (sec)
u velocity (cm/sec)
x concentration of the aqueous phase (mg/L)
X dimensionless concentration $x\backslash x_0$
y concentration of the organic phase (mg/L)
Y dimensionless concentration $y\backslash x_0$
z axial direction
Z dimensionless length, $Z = z/L$

Greek symbols
ϵ porosity of fibers
θ dimensionless time
τ average residence time (sec)

Subscripts
0 inlet
1 outlet
aq aqueous phase
o organic phase
x aqueous phase
y organic phase
z axial direction
$*$ equilibrium

ACKNOWLEDGMENTS

This work was supported by the National Natural Science Foundation of China (No. 29836130) and Tsinghua University Science Foundation.

REFERENCES

1. Chen, G.H.; Chai, X.J.; Yue, P.L.; Mi, Y.L. Treatment of Textile Desizing Wastewater by Pilot Scale Nanofiltration Membrane Separation. J. Membr. Sci. **1997**, *127*, 93–99.

2. Nirmal, J.D.; Pandya, V.P.; Desai, N.V.; Rangarajan, R. Cellulose Triacetate Membrane for Application in Plating, Fertilizer, and Textile Dye Industry Wastes. Sep. Sci. Technol. **1992**, *27*, 2083–2098.
3. Dahuron, L.; Cussler, E.L. Protein Extraction with Hollow Fibers. AIChE J. **1988**, *34*, 130–136.
4. Cardoso, M.M.; Viegas, R.M.C.; Crespo, J.P.S.G. Extraction and Re-extraction of Phenylalanine by Cationic Reversed Micelles in Hollow Fiber Contactors. J. Membr. Sci. **1999**, *156*, 303–319.
5. Stevanovic, S.M.; Mitrovic, M.V.; Korenman, Y.I. Membrane Extraction of Phenol with Linear Monoalcyl Cyclohexane. Sep. Sci. Technol. **1999**, *34*, 651–663.
6. Ilias, S.; Schimmel, K.A.; Yezek, P.M. Nondispersive Liquid–Liquid Extraction of Copper and Zinc from an Aqueous Solution by DEHPA and LIX984 in a Hollow Fiber Membrane Module. Sep. Sci. Technol. **1999**, *34*, 1007–1019.
7. George, A.; Cattrall, R.W.; Hamilton, I.C.; Kolev, S.D.; Paimin, R. The Study of a Membrane for Extraction Gold(III) from Hydrochloric Acid Solutions. J. Membr. Sci. **1998**, *138*, 279–285.
8. Tong, Y.P.; Hirata, M.; Takanashi, H. Extraction of Lactic Acid from Fermented Broth with Micorporous Hollow Fiber Membranes. J. Membr. Sci. **1998**, *143*, 81–91.
9. Chen, V.; Hlavacek, M. Application of Voronio Tessllation for Modeling Randomly Packed Hollow-Fiber Bundles. AIChE J. **1994**, *40*, 606–612.
10. Park, J.K.; Chang, H.N. Flow Distribution in the Fiber Lumen Side of a Hollow-Fiber Module. AIChE J. **1986**, *32*, 1937–1947.

Received February 2001
Revised August 2001

MARCEL DEKKER, INC.
270 Madison Avenue, New York, New York 10016

Request Permission or Order Reprints Instantly!